

Crystal structure, thermal and electrotransport properties of $\text{NdBa}_{1-x}\text{Sr}_x\text{FeCo}_{0.5}\text{Cu}_{0.5}\text{O}_{5+\delta}$ ($0.02 \leq x \leq 0.20$) solid solutions



A.I. Klyndyuk*, Ya.Yu. Zhuravleva, N.N. Gundilovich

Belarus State Technological University, 13a Sverdlova str., Minsk, 220006, Belarus Republic

* Corresponding author: klyndyuk@belstu.by

This article belongs to the regular issue.

© 2021, The Authors. This article is published in open access form under the terms and conditions of the Creative Commons Attribution (CC BY) license (<http://creativecommons.org/licenses/by/4.0/>).

Abstract

Using solid-state reactions method, the solid solutions of layered oxygen-deficient perovskites $\text{NdBa}_{1-x}\text{Sr}_x\text{FeCo}_{0.5}\text{Cu}_{0.5}\text{O}_{5+\delta}$ ($0.02 \leq x \leq 0.20$) were prepared; their crystal structure, thermal stability, thermal expansion, electrical conductivity and thermopower were studied. It was found that $\text{NdBa}_{1-x}\text{Sr}_x\text{FeCo}_{0.5}\text{Cu}_{0.5}\text{O}_{5+\delta}$ phases crystallize in tetragonal syngony (space group $P4/mmm$) and are p -type semiconductors, whose conductivity character at high temperatures changed to the metallic one due to evolution from the samples of so-called weakly-bonded oxygen. Partial substitution of barium by strontium in $\text{NdBaFeCo}_{0.5}\text{Cu}_{0.5}\text{O}_{5+\delta}$ leads to the small decreasing of unit cell parameters, thermal stability and thermopower of $\text{NdBa}_{1-x}\text{Sr}_x\text{FeCo}_{0.5}\text{Cu}_{0.5}\text{O}_{5+\delta}$ solid solutions, increasing of their electrical conductivity values and slightly affects their linear thermal expansion coefficient and activation energy of electrical transport values.

Keywords

layered perovskites
thermal stability
thermal expansion
electrical conductivity
thermopower

Received: 02.06.2021

Revised: 01.07.2021

Accepted: 08.07.2021

Available online: 08.07.2021

1. Introduction

Layered oxygen-deficient double perovskites of $\text{LnBaMe}'\text{Me}''\text{O}_{5+\delta}$ ($\text{Ln} - \text{Y}$, rare-earth element (REE), Me' , $\text{Me}'' - 3d$ -metal) have a complex of unique properties, including large values of electrical conductivity and thermopower, and contain in their structure labile oxygen, so they may be used as functional materials for different purposes: high-temperature oxide thermoelectrics, electrode materials for solid-oxide fuel cells (SOFC), materials for working elements of semiconducting chemical gas sensors, catalysts of hydrocarbons oxidation, etc. [1–6].

$\text{LnBaCo}_2\text{O}_{5+\delta}$ phases demonstrate high electrochemical performance in oxygen reduction reaction (ORR) [4–8], but values of their linear thermal expansion coefficient (TEC, α) are too large (circa $(15\text{--}29) \cdot 10^{-6} \text{ K}^{-1}$ [7–9]) in comparison to the TEC of commonly used in SOFC zirconia, ceria, or perovskite-like based solid electrolytes, which are equal to $(10\text{--}11) \cdot 10^{-6} \text{ K}^{-1}$, $(12\text{--}13) \cdot 10^{-6}$, and $(10\text{--}13) \cdot 10^{-6} \text{ K}^{-1}$ respectively [10], which limits the practical implementation of these phases as cathode materials in SOFC.

Many studies [8,9,11–18] have demonstrated that partial substitution in $\text{LnBaCo}_2\text{O}_{5+\delta}$ of cobalt by other $3d$ -metal or barium by strontium essentially improves electrochemical performance of solid solutions forming at such substitution and reduces their TEC value. So, partial substitution of cobalt by iron in $\text{LnBaCo}_2\text{O}_{5+\delta}$ ($\text{Ln} - \text{Pr}$, Nd) leads to the reducing of TEC and polarization resistance of materials forming at this substitution and also improves their long-term stability at implementation as cathode materials of SOFC [12,13,15]. Doping of barium by strontium and of cobalt by copper or iron in $\text{YBaCo}_2\text{O}_{5+\delta}$ lead to the reducing of TEC of forming solid solutions, improving of their structural stability and electrochemical performance [9,16].

So, obtaining and studying of solid solutions, including complex substituted ones, on the basis of layered oxygen-deficient double perovskites is an actual task, having scientific and practical interest.

In this work we studied the effect of partial substitution of barium by strontium in $\text{NdBaFeCo}_{0.5}\text{Cu}_{0.5}\text{O}_{5+\delta}$ on the crystal structure, thermal and electrotransport properties of $\text{NdBa}_{1-x}\text{Sr}_x\text{FeCo}_{0.5}\text{Cu}_{0.5}\text{O}_{5+\delta}$ solid solutions as perspective cathode materials for intermediate-temperature SOFC.

2. Experimental

Ceramic samples of $\text{NdBa}_{1-x}\text{Sr}_x\text{FeCo}_{0.5}\text{Cu}_{0.5}\text{O}_{5+\delta}$ ($x = 0.02, 0.05, 0.10, \text{ and } 0.20$) solid solutions were prepared by means of solid-state reactions method from Nd_2O_3 (NO-L), BaCO_3 (pure), SrCO_3 (pure), Fe_2O_3 (super pure 2-4), Co_3O_4 (pure), and CuO (pure for analysis) in air at temperature of 1173 K within 40 h with consequent sintering during 9–18 h in air at temperatures of 1223–1273 K according to the methods, described in [19,20].

Identification of the samples and determination of their lattice constants was performed by means of X-ray diffraction analysis (XRD) (X-ray diffractometer Bruker D8 Advance XRD, Cu $K\alpha$ -radiation). IR-absorption spectra of powders were recorded in the mixtures with KBr within 300–1500 cm^{-1} (ThermoNicolet Nexus Fourier-Transform Infrared Spectrometer). Apparent (effective) density of the sintered ceramics (ρ_{eff}) was determined from the mass and dimensions of the samples, and their porosity (Π) was calculated using Eq. (1):

$$\Pi = (1 - \rho_{\text{eff}}/\rho_{\text{XRD}}) \cdot 100\%, \quad (1)$$

where ρ_{XRD} – X-ray density of the samples.

Thermal stability of the powdered samples was studied by means of thermoanalytical system of TGA/DSC-1/1600 HF in air within 300–1100 K temperature interval. Thermal expansion of the sintered ceramics was investigated using DIL 402 PC quartz dilatometer in air within temperature interval of 300–1100 K [21]. Electrical conductivity and thermopower of $\text{NdBa}_{1-x}\text{Sr}_x\text{FeCo}_{0.5}\text{Cu}_{0.5}\text{O}_{5+\delta}$ solid solutions were studied in air within 300–1100 K according to the methods, described in detail in [20]. Values of TEC and apparent activation energies of electrical conductivity (E_A) and thermopower (E_S) were calculated from the linear parts of

$\Delta l/l_0 = f(T)$, $\ln(\sigma \cdot T) = f(1/T)$, and $S = f(1/T)$ dependences, respectively.

3. Results and Discussion

After final stage of the synthesis, all the samples of the $\text{NdBa}_{1-x}\text{Sr}_x\text{FeCo}_{0.5}\text{Cu}_{0.5}\text{O}_{5+\delta}$ solid solutions were single phase, within XRD accuracy (Fig. 1a), and had a structure of tetragonally distorted double perovskite of YBaCuFeO_5 type ($a \approx a_p, c \approx 2a_p$) [1], and their reflections were indexed in the framework of the $P4/mmm$ space group with unit cell parameters of $a = 3.903\text{--}3.914 \text{ \AA}$ and $c = 7.707\text{--}7.715 \text{ \AA}$ (Table 1).

As can be seen from the Table 1, increasing of the substitution degree of larger Ba^{2+} ion by smaller Sr^{2+} one (for C.N. = 12 $R(\text{Ba}^{2+}) = 1.60 \text{ \AA}$, $R(\text{Sr}^{2+}) = 1.44 \text{ \AA}$ [22]) leads to the decreasing of the size of the unit cell of the $\text{NdBa}_{1-x}\text{Sr}_x\text{FeCo}_{0.5}\text{Cu}_{0.5}\text{O}_{5+\delta}$ phases. Porosity of the sintered ceramics enlarged at x increasing (Table 1), which let us conclude that partial substitution of barium by strontium in $\text{NdBaFeCo}_{0.5}\text{Cu}_{0.5}\text{O}_{5+\delta}$ slightly reduces sinterability of this perovskite.

On the IR-absorption spectra of the samples were detected some absorption bands with extrema at 351–353 cm^{-1} (ν_1), 467–470 cm^{-1} (ν_2), 576–582 cm^{-1} (ν_3), and 660–665 cm^{-1} (ν_4) (Fig. 1b), which were attributed, according to [23], to the stretching (ν_3, ν_4) and bending vibrations (ν_1) of the (Fe,Co,Cu)–O–(Fe,Co,Cu) bonds in the [(Fe,Co,Cu)O₂] basal planes (ν_1, ν_3), as well as stretching vibrations of apical oxygen of (Fe,Co,Cu)–O–(Fe,Co,Cu) bonds along c axis (ν_4) in the structure of $\text{NdBa}_{1-x}\text{Sr}_x\text{FeCo}_{0.5}\text{Cu}_{0.5}\text{O}_{5+\delta}$ phases. At x increasing the ν_3 and ν_4 bands shifted to the larger values,

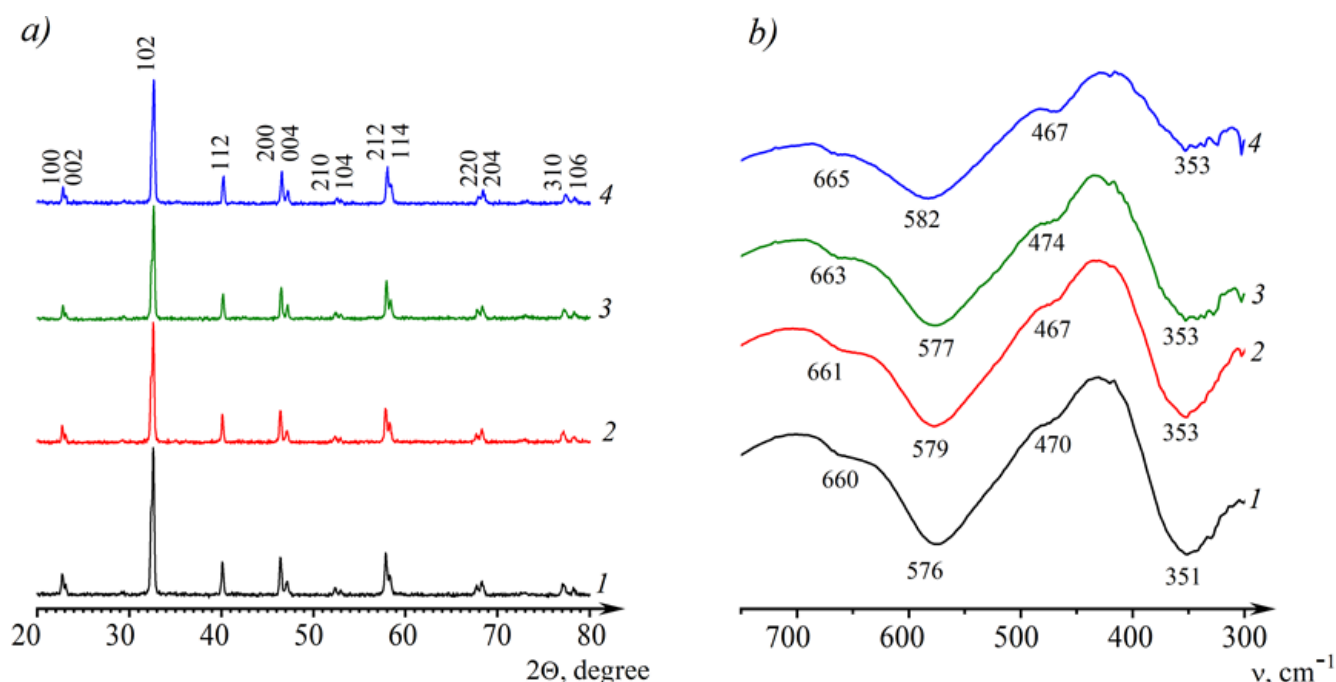


Fig. 1 X-ray powder diffractograms (a) and IR-absorption spectra (b) of $\text{NdBa}_{1-x}\text{Sr}_x\text{FeCo}_{0.5}\text{Cu}_{0.5}\text{O}_{5+\delta}$ solid solutions: $x = 0.02$ (1); 0.05 (2); 0.10 (3); 0.20 (4)

Table 1 The unit cell parameters (*a*, *c*, *c/2a*, *V*), effective density (ρ_{eff}) and porosity (Π) of NdBa_{1-x}Sr_xFeCo_{0.5}Cu_{0.5}O_{5+δ} layered perovskites finally sintered at 1273 K

<i>x</i>	<i>a</i> , Å	<i>c</i> , Å	<i>c/2a</i> , Å	<i>V</i> , Å ³	ρ_{eff} , g/cm ³	Π , %
0.02	3.913(1)	7.715(1)	0.9860	118.1(1)	5.54	10
0.05	3.914(1)	7.711(1)	0.9851	118.1(1)	5.62	8
0.10	3.911(2)	7.707(2)	0.9853	117.9(1)	5.54	12
0.20	3.903(1)	7.708(1)	0.9876	117.5(1)	4.84	21

which pointed out to increasing of energy of metal–oxygen interactions in the crystal structure of these phases. Results of IR-absorption spectroscopy correlate with the XRD results, showing that increasing of substitution degree of barium by strontium in NdBa_{1-x}Sr_xFeCo_{0.5}Cu_{0.5}O_{5+δ} solid solutions leads to the shrinking of their unit cell.

According to the results of thermal analysis, near the room temperature all the samples were thermally stable, but, beginning from the temperatures of 623–663 K (*T_b*) the small mass loss (0.6–0.8%) was detected (Fig. 2a), which took place due to the evolution of the labile (weakly-bonded) oxygen from the samples into environment [24]. Values of *T_b* decreased at *x* increasing (Fig. 2c, Table 2), which indicated increasing of mobility of weakly-bonded oxygen in the structure of NdBa_{1-x}Sr_xFeCo_{0.5}Cu_{0.5}O_{5+δ} solid solutions at increasing of substitution degree of barium by strontium. On the temperature dependences of the relative elongation ($\Delta l/l_0$) of materials studied an anomaly in a kink near *T_k* = 640–680 K accompanied by the increase the TEC value was detected (Fig. 2b, Table 2), which took place due to the rearrangement of oxygen sublattice of the samples with consequent evolution of oxygen from them in air [24]. TEC values of ceramics in high-temperature region (α_{HT} , *T* > *T_k*) were 15–24% larger than in the low-temperature

one (α_{LT} , *T* < *T_k*) (Table 3). Values of TEC of NdBa_{1-x}Sr_xFeCo_{0.5}Cu_{0.5}O_{5+δ} solid solutions in both temperature regions slightly varied but temperature of anomaly (*T_k*) essentially decreased (Fig. 2d) at *x* increasing.

As can be seen from the data given in the Fig. 3a,b, materials studied are *p*-type (*S* > *o*) semiconductors ($\partial\sigma/\partial T > 0$). Their conductivity character at high temperatures (*T* > *T_{max}*) changed to the metallic one ($\partial\sigma/\partial T < 0$), which was accompanied by the change of the sign of the $\partial S/\partial T$ derivative ($\partial S/\partial T < 0$ at *T* < *T_{min}* and $\partial S/\partial T > 0$ at *T* > *T_{min}*). Observed anomalies of electrotransport properties of NdBa_{1-x}Sr_xFeCo_{0.5}Cu_{0.5}O_{5+δ} phases as well as described earlier anomaly of thermal expansion were due to the evolution of the weakly-bonded oxygen from the samples [24]. Note that temperatures of σ and *S* anomalies, *T_{max}* and *T_{min}* respectively, at *x* increasing shifted to the smaller temperatures (Fig. 3c,d, Table 2) like *T_b* and *T_k* temperatures. It is interesting that values of *T_b*, *T_k* and *T_{min}* temperatures were rather close to each other, but *T_{max}* value was essentially larger (Table 2, Figs. 2c,d, 3c,d). Values of all critical temperatures (*T_{cr}*: *T_b*, *T_k*, *T_{max}*, and *T_{min}*) decrease at increasing of strontium content in the NdBa_{1-x}Sr_xFeCo_{0.5}Cu_{0.5}O_{5+δ} solid solutions, hereby dependence *T_{cr}* = *f*(*x*) was almost linear for *T_k*, underlinear for *T_b* and *T_{min}*, and overlinear for *T_{max}* increased despite of the

Table 2 Values of critical temperatures (*T_b*, *T_k*, *T_{max}*, and *T_{min}*) of NdBa_{1-x}Sr_xFeCo_{0.5}Cu_{0.5}O_{5+δ} ceramics

<i>x</i>	<i>T_b</i> , K	<i>T_k</i> , K	<i>T_{max}</i> , K	<i>T_{min}</i> , K
0.02	663	680	734	685
0.05	631	670	733	665
0.10	631	660	730	650
0.20	623	640	709	650

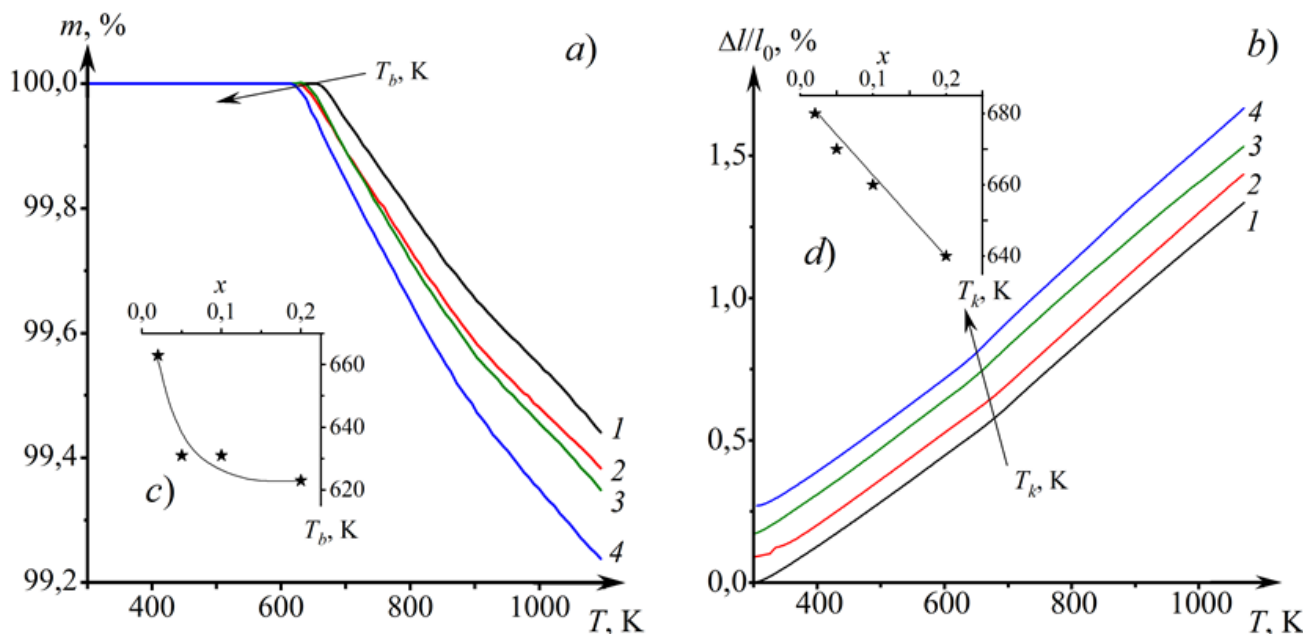


Fig. 2 Temperature dependences of mass loss (a) and relative elongation (b) of NdBa_{1-x}Sr_xFeCo_{0.5}Cu_{0.5}O_{5+δ} samples: *x* = 0.02 (1); 0.05 (2); 0.10 (3); 0.20 (4). Dilatometric curves are shifted from each other by 0.1% for the clarity of presentation. Insets shows concentration dependences of temperatures of mass loss onset (c) and kink of the $\Delta l/l_0 = f(T)$ dependences (d)

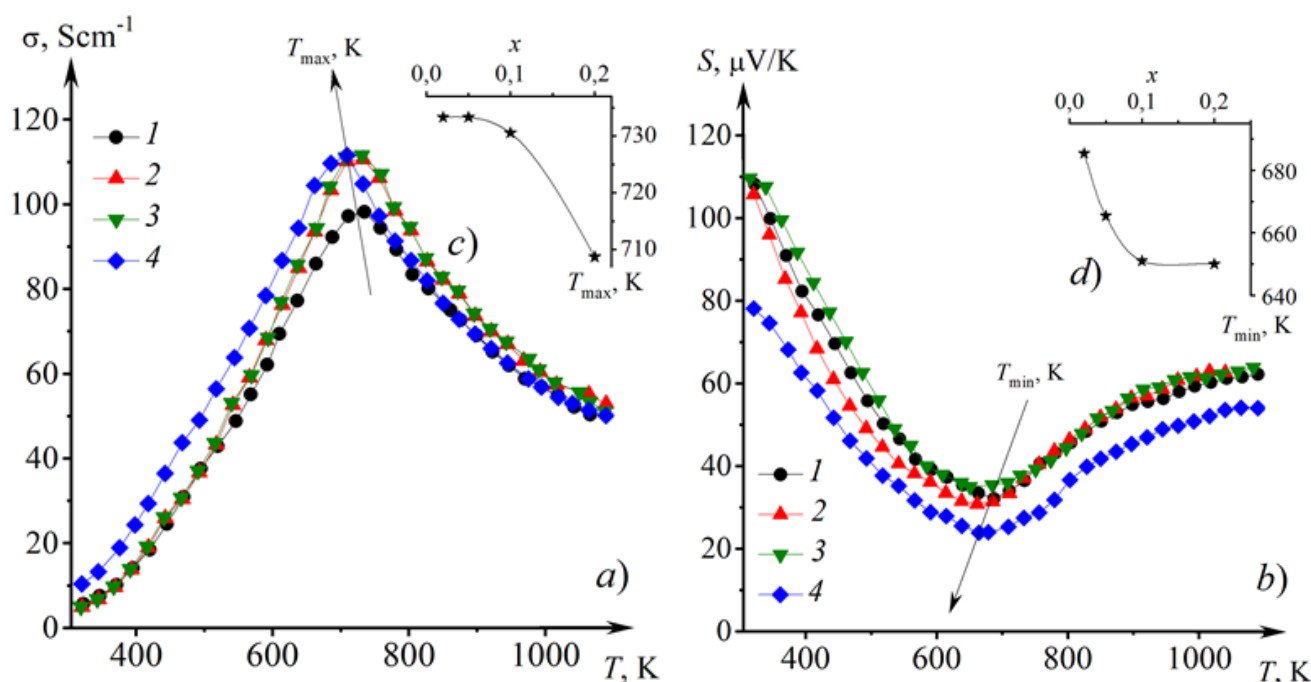


Fig. 3 Temperature dependences of electrical conductivity (a) and thermo-EMF coefficient (b) of $\text{NdBa}_{1-x}\text{Sr}_x\text{FeCo}_{0.5}\text{Cu}_{0.5}\text{O}_{5+\delta}$ sintered ceramics: $x = 0.02$ (1); 0.05 (2); 0.10 (3); 0.20 (4). Insets shows concentration dependences of temperatures of maximum on the $\sigma = f(T)$ dependences (c) and minimum of the $S = f(T)$ dependences (d)

fact that porosity of the samples enlarged at increasing of strontium content (Table 1). So, our results show that partial substitution of barium by strontium in $\text{NdBaFeCo}_{0.5}\text{Cu}_{0.5}\text{O}_{5+\delta}$ is an effective way to increase its electrical conductivity.

Layered oxygen-deficient double perovskites $\text{LnBaMe}'\text{Me}''\text{O}_{5+\delta}$ possess polaronic character of charge transfer [1,19,24], and temperature dependences of their electrical conductivity and thermopower obey Eqs. (2-3)

$$\sigma = (A/T) \cdot \exp(-E_A/kT), \tag{2}$$

$$S = (k/e) \cdot (-E_S/kT + B), \tag{3}$$

where $E_A = E_S + E_m$ and E_S - activation energies of electrical conductivity and thermopower respectively, E_S is also activation energy of charge carriers - polarons, and E_m is energy of their transfer [25].

As can be seen from the data given in the Table 3, values of energies of activation of electrical transport, in the whole, slightly varied at varying strontium content in the samples. Comparing obtained in this work results with the data of [24], where for $\text{NdBaFeCo}_{0.5}\text{Cu}_{0.5}\text{O}_{5+\delta}$ layered perovskite was found that $E_A = 0.245$ eV, $E_S = 0.048$ eV, and $E_m = 0.200$ eV, we can conclude that partial substitution

of barium by strontium in this parent phase does not affect practically the value of activation energy of charge carriers - polarons, but results in essential reducing of transfer energy of charge carriers.

4. Conclusions

By means of solid-state reactions method the ceramic samples of $\text{NdBa}_{1-x}\text{Sr}_x\text{FeCo}_{0.5}\text{Cu}_{0.5}\text{O}_{5+\delta}$ ($x = 0.02, 0.05, 0.10,$ and 0.20) solid solutions were prepared, and their crystal structure and physico-chemical properties were studied. It was found that obtained materials had tetragonal structure, whose unit cell parameters slightly depend on their cationic composition, and are p-type semiconductors, whose conductivity character changes to the metallic one at high temperatures due to the evolution of oxygen from their crystal structure into environment. It was established that partial substitution of barium by strontium in $\text{NdBaFeCo}_{0.5}\text{Cu}_{0.5}\text{O}_{5+\delta}$ results in the increasing of electrical conductivity, reducing of energy activation of electrical conductivity, thermopower and thermal stability of solid solutions forming at this substitution $\text{NdBa}_{1-x}\text{Sr}_x\text{FeCo}_{0.5}\text{Cu}_{0.5}\text{O}_{5+\delta}$.

Table 3 Values of TEC (α) and apparent activation energy of electrical transport (E_o, E_s, E_m) for the sintered $\text{NdBa}_{1-x}\text{Sr}_x\text{FeCo}_{0.5}\text{Cu}_{0.5}\text{O}_{5+\delta}$ ceramics

x	$10^6 \cdot \alpha$		$E_o, \text{ eV}$ (350-700 K)	$E_s, \text{ eV}$ (400-650 K)	$E_m, \text{ eV}$
	$\alpha_{LT}, \text{ K}^{-1}$	$\alpha_{HT}, \text{ K}^{-1}$			
0.02	15.8	19.3	0.190	0.047	0.143
0.05	16.3	20.0	0.203	0.044	0.159
0.10	16.6	19.1	0.200	0.054	0.146
0.20	16.4	20.4	0.167	0.038	0.129

References

1. Klyndyuk AI. Perovskite-like Oxides o112 Type: Srtucture, Properties and Possible Applications. Advances in Chemistry Research. V. 5. Ed. by J.C. Taylor. Nova Sci Publ: New-York; 2010. P. 59-105.
2. Lyagaeva J, Danilov N, Tarutin A, Vdovin G, Medvedev D, Demin A, Tsiakaras P. Designing a protonic ceramic fuel cell with novel electrochemically active oxygen electrodes based

- on doped $\text{Nd}_{0.5}\text{Ba}_{0.5}\text{FeO}_{3-\delta}$. Dalton Trans. 2018;47(24):8149–8157. doi:[10.1039/c8dt01511b](https://doi.org/10.1039/c8dt01511b)
3. Tsvetkov DS, Ivanov IL, Malyshev DA, Sednev AL, Sereda VV, Zuev AY. Double perovskites $\text{REBaCo}_{2-x}\text{M}_x\text{O}_{6-\delta}$ (RE = La, Pr, Nd, Eu, Gd, Y; M = Fe, Mn) as energy-related materials: an overview. Pure Appl Chem. 2019;19(6):923–940. doi:[10.1515/pac-2018-1103](https://doi.org/10.1515/pac-2018-1103)
 4. Afroze S, Karim AK, Cheok Q, Eriksson S, Azad AK. Latest development of double perovskite electrode materials for solid oxide fuel cell: a review. Front Energy. 2019;13:770–897. doi:[10.1007/s1708-019-0651-x](https://doi.org/10.1007/s1708-019-0651-x)
 5. Kaur P, Singh C. Review of perovskite-structure related cathode materials for solid oxide fuel cell. Ceramics International. 2020;46(5):5521–5535. doi:[10.1016/j.ceramint.2019.11.066](https://doi.org/10.1016/j.ceramint.2019.11.066)
 6. Istomin SYa, Lyskov NV, Mazo GN, Antipov EV. Electrode materials based on complex *d*-metal oxides for symmetrical solid oxide fuel cell. Russ Chem Rev. 2021;90(6):644–676. doi:[10.1070/RCR4979](https://doi.org/10.1070/RCR4979)
 7. Kim J-H, Manthiram A. Layered $\text{LnBaCo}_2\text{O}_{5+\delta}$ oxides as cathodes for intermediate-temperature solid oxide fuel cell. J Electrochem Soc. 2008;155:3385. doi:[10.1149/1.2839028](https://doi.org/10.1149/1.2839028)
 8. Kim J-H, Manthiram A. Layered $\text{LnBaCo}_2\text{O}_{5+\delta}$ perovskite cathodes for solid oxide fuel cells: an overview and perspective. J Mater Chem. 2015;3:24195–24210. doi:[10.1039/C5TA06212A](https://doi.org/10.1039/C5TA06212A)
 9. Lin Y, Jin F, Yang X, Nik B, Li Y, He T. $\text{YBaCo}_2\text{O}_{5+\delta}$ -based double perovskite cathodes for intermediate-temperature solid oxide fuel cells with simultaneously improved structural stability and thermal expansion properties. Electrochim Acta. 2019;297:344–454. doi:[10.1016/j.electacta.2018.11.214](https://doi.org/10.1016/j.electacta.2018.11.214)
 10. Kharton V, Marques F, Atkinson A. Transport properties of solid oxide electrolyte ceramics: a brief review. Solid State Ionics. 2004;174:135–149. doi:[10.1016/j.ssi.2004.06.015](https://doi.org/10.1016/j.ssi.2004.06.015)
 11. Xue J, Shen Y, He T. Performance of double-perovskite $\text{YBa}_{0.5}\text{Sr}_{0.5}\text{Co}_2\text{O}_{5+\delta}$ as cathode material for intermediate-temperature solid oxide fuel cells. Int J Hydrog Energy. 2011;36:6894–6898. doi:[10.1016/j.ijhydene.2011.02.090](https://doi.org/10.1016/j.ijhydene.2011.02.090)
 12. Cherepanov VA, Aksenova TV, Gavrilova LY, Mikhaleva KN. Structure, nonstoichiometry and thermal expansion of $\text{NdBa}(\text{Co},\text{Fe})_2\text{O}_{5+\delta}$ layered perovskites. Solid State Ionics. 2011;188:53–87. doi:[10.1016/j.ssi.2010.10.021](https://doi.org/10.1016/j.ssi.2010.10.021)
 13. Zhang S-L, Chen K, Zhang A-P, Li C-X, Li C-Y. Effect of Fe doping on the performance of suspension plasma-sprayed $\text{PrBa}_{0.5}\text{Sr}_{0.5}\text{Co}_{2-x}\text{Fe}_x\text{O}_{5+\delta}$ cathodes for intermediate-temperature solid oxide fuel cells. Ceramics International. 2017;43:11648–11655. doi:[10.1016/j.ceramint.2017.05.438](https://doi.org/10.1016/j.ceramint.2017.05.438)
 14. Jin F, Li Y, Wang Y, Chu X, Xu M, Zhai Y, Zhang Y, Fang W, Zou P, He T. Evaluation of Fe and Mn co-doped layered perovskite $\text{PrBaCo}_{2/3}\text{Fe}_{2/3}\text{Mn}_{1/2}\text{O}_{5+\delta}$ as a novel cathode for intermediate-temperature solid oxide fuel cells. Ceramics International. 2018;44:22489–22496. doi:[10.1016/j.ceramint.2018.09.018](https://doi.org/10.1016/j.ceramint.2018.09.018)
 15. Cordaro G, Donazzi A, Pelosato R, Mastropasqua L, Cristiani C, Sora IN, Dotelli G. Structural and Electrochemical Characterization of $\text{NdBa}_{1-x}\text{Co}_{2-y}\text{Fe}_y\text{O}_{5+\delta}$ as Cathode for Intermediate Temperature Solid Oxide Fuel Cells. J Electrochem Soc. 2020;167:024502. doi:[10.1149/1945-7111/ab628b](https://doi.org/10.1149/1945-7111/ab628b)
 16. Klyndyuk AI, Mosialek M, Kharitonov DS, Chizhova EA, Zimovska M, Socha RP, Komenda A. Structural and electrochemical characterization of $\text{YBa}(\text{Fe},\text{Co},\text{Cu})_2\text{O}_{5+\delta}$ layered perovskites as cathode materials for solid oxide fuel cells. Int J Hydrog Energy. 2021;46(32):16977–16988. doi:[10.1016/j.ijhydene.2021.01.141](https://doi.org/10.1016/j.ijhydene.2021.01.141)
 17. Yao C., Yang J., Zhang H., Chen S., Lang X, Meng J, Cai K. Evaluation of A-site Ba-deficient $\text{PrBa}_{0.5-x}\text{Sr}_{0.5}\text{Co}_2\text{O}_{5+\delta}$ ($x = 0, 0.04, \text{ and } 0.08$) as cathode materials for solid oxide fuel cells. J Alloys Compd. 2021;883:160759. doi:[10.1016/j.jallcom.2021.160759](https://doi.org/10.1016/j.jallcom.2021.160759)
 18. Yang Q, Tian D, Liu R, Wu H, Chan Y, Ding Y, Lu X, Lin B. Exploiting rare-earth-abundant layered perovskite cathodes of $\text{LnBa}_{0.5}\text{Sr}_{0.5}\text{Co}_{1.5}\text{Fe}_{0.5}\text{O}_{5+\delta}$ (Ln = La and Nd) for SOFC. Int J Hydrog Energy. 2021;46(7):5630–5642. doi:[10.1016/j.ijhydene.2020.11.031](https://doi.org/10.1016/j.ijhydene.2020.11.031)
 19. Klyndyuk AI, Chizhova EA. Crystal structure, Thermal Expansion, and Electrical Properties of Layered $\text{LaBa}(\text{Fe},\text{Co},\text{Cu})_2\text{O}_{5+\delta}$ (Ln = Nd, Sm, Gd) Oxides. Glass Phys Chem. 2014;40(1):124–128. doi:[10.1134/S10876595961401012X](https://doi.org/10.1134/S10876595961401012X)
 20. Klyndyuk AI, Chizhova EA. Structure, Thermal Expansion, and Electrical Properties of BiFeO_3 - NdMnO_3 Solid Solutions. Inorg Mater. 2015;51(3):272–277. doi:[10.1134/S0020168515020090](https://doi.org/10.1134/S0020168515020090)
 21. Klyndyuk AI, Chizhova EA, Poznyak AI. Preparation and Characterization of $\text{Bi}_{4-x}\text{Pr}_x\text{Ti}_3\text{O}_{10}$ Solid Solutions. Chimica Techno Acta. 2017;4(4):211–217. doi:[10.15826/chimtech/2017.4.4.01](https://doi.org/10.15826/chimtech/2017.4.4.01)
 22. Shannon RD. Revised effective ionic radii and systematic studies of interatomic distances in halides and chalcogenides. Acta Cryst. 1976;32:751–767. doi:[10.1107/S0567739476001551](https://doi.org/10.1107/S0567739476001551)
 23. Atanassova YK, Popov VN, Bogachev GG, Iliev MN, Mitros C, Psycharis V, Pissas M. Raman- and infrared active phonons in YBaCuFeO_5 : experimental and lattice dynamics. Phys Rev B. 1993;47:15201–15207. doi:[10.1103/PhysRevB.47.15201](https://doi.org/10.1103/PhysRevB.47.15201)
 24. Klyndyuk AI, Chizhova EA. Physicochemical Properties of $\text{La}(\text{Ba},\text{M})\text{CuFeO}_{5+\delta}$ (M = Sr, Ca, Mg) solid solutions. Inorg Mater. 2006;42(4):436–442. doi:[10.1134/S0020168506040182](https://doi.org/10.1134/S0020168506040182)
 25. Mott NF, Davis EA. Electronic Processes in Non-Crystalline Materials. 2nd ed. New York, USA: Oxford University Press. 1979. 605 p.